Correlation between the Onset of the East Asian Subtropical Summer Monsoon and the Eastward Propagation of the Madden–Julian Oscillation

YANZHEN CHI

Fujian Meteorological Bureau, Fuzhou, China, and Department of Meteorology, The Pennsylvania State University, University Park, Pennsylvania, and Nanjing University of Information Science and Technology, Nanjing, China

FUQING ZHANG AND WEI LI

Department of Meteorology, The Pennsylvania State University, University Park, Pennsylvania

JINHAI HE AND ZHAOYONG GUAN

Nanjing University of Information Science and Technology, Nanjing, China

(Manuscript received 14 February 2014, in final form 22 October 2014)

ABSTRACT

Using the daily outgoing longwave radiation (OLR), the pentad Climate Prediction Center Merged Analysis of Precipitation (CMAP), and the 6-h Climate Forecast System Reanalysis (CFSR) dataset from 1979 to 2010, a composite analysis along with space–time wave filtering is performed to examine the linkage between the Madden–Julian oscillation (MJO) and the onset of the East Asian subtropical summer monsoon (EASSM) (over 20°–30°N, 110°–120°E). The onset of the EASSM is shown to be best characterized by the reversal of the mean meridional wind shear related to the rapid reestablishment of the South Asian high (SAH) over the southern Indochinese Peninsula in the upper troposphere. The mean date of EASMM onset is near the end of April, which is about a month earlier than the typical onset of the East Asian summer monsoon. Further analysis indicates that the onset of the EASSM and the reestablishment of SAH are often associated with the arrival of the wet phase of the tropical MJO over the central and eastern Indian Ocean.

1. Introduction

The Asian summer monsoon system has two components: the South Asian summer monsoon (or Indian summer monsoon) and the East Asian summer monsoon (EASM). The latter is one of the most prominent phenomena associated with the seasonal variation of the atmospheric circulation in the Northern Hemisphere. The EASM is commonly further divided into two branches: (i) a tropical branch, comprising the South China Sea summer monsoon and the western North Pacific summer monsoon, and (ii) a subtropical branch, which is commonly referred to as the East Asian subtropical summer monsoon (EASSM) and covers mainland China and the Japanese Islands (Zhu et al. 1986; Tao and Chen 1987; Wang and LinHo 2002; He et al. 2007). Adapted from the schematic of Wang and LinHo (2002), Fig. 1 shows the division and subdivisions of the Asian summer monsoon. The establishment, evolution, and multiscale variability of the EASM and its interactions with South Asian summer monsoon and ENSO have attracted enormous attention (e.g., Wang et al. 2000; Chang et al. 2004). Tropical forcing, midlatitude baroclinic systems, diabatic heating over the Tibetan Plateau, and air–sea interaction have all been identified as influencing the onset and variability of the EASM (e.g., Chang and Chen 1995; Chan et al. 2000; Ding and Liu 2001; Zhang et al. 2004; Ding and Chan 2005; Wu et al. 2012).

Earlier works of Tao and Chen (1987), Ding (1994), and Lau and Yang (1997) suggested that the EASM begins in mid-May over the South China Sea (SCS), while Qian and Lee (2000) and Ding and Chan (2005) argued that onset of the EASM is over the Indochinese Peninsula earlier in May. More recently, Qian et al. (2005)

Corresponding author address: Professor Fuqing Zhang, Department of Meteorology, The Pennsylvania State University, 503 Walker Bldg., University Park, PA 16802.
E-mail: fzhang@psu.edu

DOI: 10.1175/JAS-D-14-0038.1

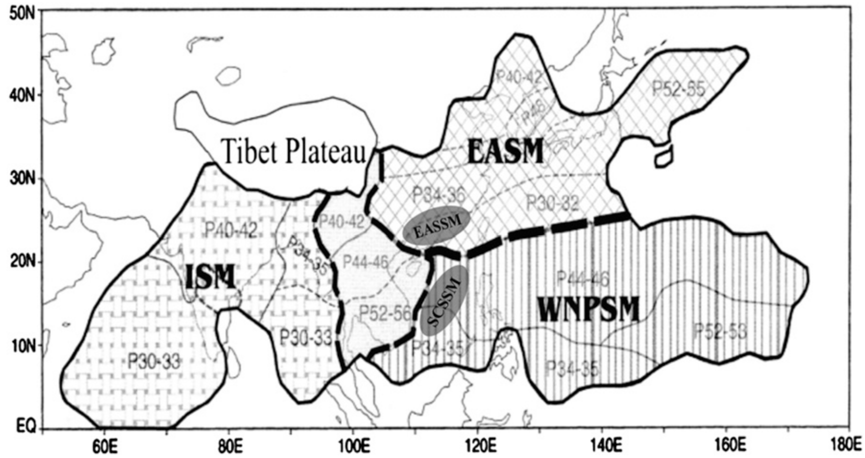

FIG. 1. Schematic depiction for the division of the Asian summer monsoon adapted from Wang and LinHo (2002). Divisions shown are the Indian summer monsoon (ISM), East Asian summer monsoon (EASM), South China Sea summer monsoon (SCSSM), East Asian Subtropical summer monsoon (EASSM), and western North Pacific summer monsoon (WNPSM). The numbers denote the timing of local peak monsoon rainfall in Julian pentads.

proposed that the Asian summer monsoon simultaneously establishes over northern SCS, the Indochinese Peninsula, and the Bay of Bengal.

Most of these aforementioned studies regarded the EASSM as the northward propagation of the tropical summer monsoon. However, some have shown that the subtropical rain belt over East Asia in late March–April (Tian and Yasunari 1998; Wan and Wu 2007) shares some common features of a typical monsoon phenomenon and should be treated as the onset of the quasi-independent EASSM (Chen et al. 2000; Xu and Zhu 2002; He et al. 2008; Ren et al. 2010). Wang et al. (2004) showed that the onset of the SCS summer monsoon is associated with a strengthening of the mean 850-hPa westerly wind over the central SCS (5°–15°N, 110°–120°E). In contrast, the onset of the EASSM has been demonstrated to be associated with the strengthening of the mean southerly wind due to the reversal of zonal land–sea thermal contrast (Qi et al. 2008; Zhao et al. 2007; Zhu et al. 2012). Through all of this debate on mechanism, there is not yet a consensus criterion for defining the EASSM onset.

In recent years, the impacts of intraseasonal oscillations in convective activity, such as the Madden–Julian oscillation (MJO) (Madden and Julian 1971), on the EASM has attracted a lot of attention (Wen et al. 2004; Ding and Chan 2005; Zhou and Chan 2005, 2013; Straub et al. 2006; Tong et al. 2009; Li et al. 2013; Lau and Waliser 2012). However, most of the aforementioned studies focus on the tropical monsoons with little attention to the subtropical monsoons, such as the EASSM.

The current study seeks to identify key changes in the atmospheric circulation that can be used to best define the onset of the EASSM and to examine the association between the tropical MJO activities and the onset of the EASSM. Section 2 introduces the dataset and methodology of the current study. Section 3 seeks to establish an index for defining the onset of the EASSM. Section 4 links the MJO activities to the onset of the EASSM. Concluding remarks are given in section 5.

2. Data and methods

The primary dataset analyzed in this study is the National Centers for Environmental Prediction (NCEP) Climate Forecast System (CFS) Reanalysis (Saha et al. 2010). The CFS Reanalysis has a horizontal resolution of 0.5° × 0.5°, with 37 vertical layers available every 6 h. The daily National Oceanographic and Atmospheric Administration (NOAA) outgoing longwave radiation (OLR) (Liebmann and Smith 1996) is used as a proxy for convective activity, while the Julian pentad precipitation dataset comes from the Climate Prediction Center (CPC) Merged Analysis of Precipitation (CMAP; Xie and Arkin 1997), which has a horizontal resolution of 2.5° × 2.5°. All data have global coverage for the analysis period of 1979–2010.

An EASSM onset–relative composite is created for this 32-yr period of data. The pentad (which, here, is the number of 5-day periods since 1 January) of EASSM onset in each year is determined, the mean onset pentad is calculated, and all years are time shifted such that the EASSM onset is during the mean onset pentad. This mean onset date can be denoted as pentad 0 with negative (positive) pentads being before (after) onset.

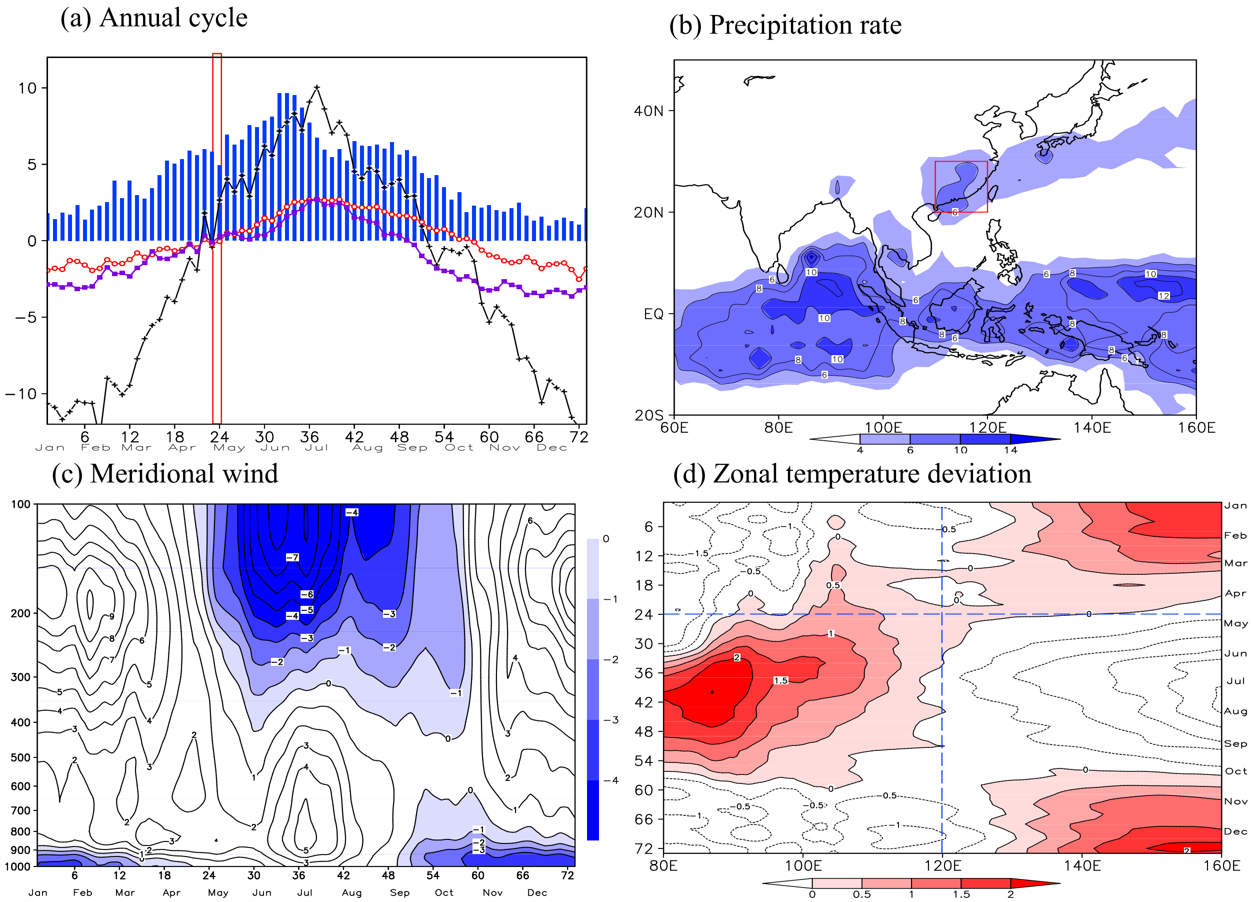

FIG. 2. (a) Annual cycle of the CMAP precipitation rate (bars, mm day^{-1}), the meridional wind shear (MWS) between 925 and 200 hPa (line with crosses, m s^{-1}), surface meridional wind (line with rectangles, m s^{-1}), and the 500-hPa zonal temperature deviation (line with circles, K) averaged over the EASSM domain. (b) CMAP precipitation rate (mm day^{-1}) averaged from the twenty-fourth to twenty-fifth pentads (>6 mm day^{-1}, contoured every 2 mm day^{-1}). (c) Height–time Hovmöller diagram of averaged meridional wind over the EASSM domain (every 1 m s^{-1}, negative values shaded). (d) Longitude–time Hovmöller diagram of zonal temperature deviation at 500 hPa over 20°–30°N (every 0.5 K, positive values shaded). The time unit is the Julian pentad.

The spatial–temporal wave-filtering method of Wheeler and Kiladis (1999) is applied to the fields of each individual year to create composite anomalies of the OLR, horizontal wind, geopotential height, and air temperature (using fields on standard isobaric levels). To further connect the MJO activities with the EASSM onset, the wave filtering is done using periods of 20–70 days and zonal wavenumbers 1–7 as the MJO-filtering band (qualitatively, the results are not sensitive to the selected cutoff periods so long as they include the periods between 30 and 60 days).

3. The onset of East Asian subtropical summer monsoon

As stated in Zhu et al. (2011), the latitude of 20°N can be used to empirically divide the tropical and subtropical monsoon domain over East Asia. Since the exact boundaries of the subtropical East Asian region vary in literature, the current study narrowly selects the area bounded by 20°–30°N, 110°–120°E and as the focus area of the EASSM for simplicity.[1]

To obtain a robust index for the onset of the EASSM, we first derive the climatological-mean annual cycles (using 30-yr averages from 1981 to 2010) for the CMAP precipitation rate, the meridional wind shear between 925 and 200 hPa, the surface meridional wind, and the 500-hPa zonal temperature deviation averaged over the EASSM domain (Fig. 2a). The zonal temperature deviation is defined as the anomalies relative to the zonal

[1] There is some subjectivity in the selection and definition of the EASSM region, which would have implications on the exact timing of the EASSM onset, but the physical processes that we describe here should remain valid regardless of the criteria that we used.

mean of 80°–160°E. Significant features seen in these annual cycles are the reversal of the meridional wind shear, the surface meridional wind, and the zonal air temperature deviation at around the twenty-fourth pentad (i.e., 26–30 April); by this time, the mean rainfall rate exceeds 5 mm day^{-1}. Moreover, the twenty-fourth-to-twenty-fifth-pentad-mean precipitation map indicates that the center of the area in which rainfall exceeds 6 mm day^{-1} (often regarded as a signal for significant convective precipitation) is within the focus EASSM region, and the rainfall is much heavier than in the adjacent regions, such as the South China Sea, the Indochinese Peninsula, and the Indian Peninsula (Fig. 2b). Figure 2c shows that the reversal of the meridional wind shear around the twenty-fourth pentad comes primarily from the reversal of upper-tropospheric mean meridional wind from southerly to northerly, as southerly low-level (e.g., 850-hPa) winds are seen even before the eighteenth pentad. The corresponding reversal of the zonal temperature deviation averaged over 20°–30°N (Fig. 2d) is consistent with earlier studies that had suggested that EASSM onset is induced by the zonal land–sea thermal contrast reversal (He et al. 2007; Zhao et al. 2007).

Figure 3 shows the establishment of a monsoonal meridional cell over East Asia as the mean meridional circulation reverses from the eighteenth to twenty-eighth pentads. A typical Hadley cell with ascent in the equator and descent in the subtropics persists before the twenty-fourth pentad, but the cell breaks down at the twenty-fourth pentad as the upper-tropospheric winds reverse from southerly to northerly. The establishment of a meridional cell with ascent in the subtropical and descent in the SCS area indicates the full onset of the EASSM, which is consistent with Zhu et al. (2000). As these changes in the vertical circulation take place, the intensity of the subtropical westerly jet gradually weakens. Finally, an intimate linkage of the reversal of the meridional wind shear and an abrupt westward propagation of the South Asia high (SAH) from the eastern Philippines to the southern tip of the Indochinese Peninsula can be seen in the evolution of mean streamlines at 200 hPa (Figs. 4a–f).

Based on the above analysis, we believe that the reversal of the meridional winds in both the upper and lower troposphere is strongly associated with the EASSM onset. Since the reversal of the vertical meridional wind shear can indicate the establishment of the monsoonal cell, it can be used as a key factor to define the EASSM onset. Based on the domain-averaged vertical wind shear reversal (Fig. 2a), the twenty-fourth pentad is identified here as the climatological EASSM onset date. In other words, the seasonal transition from winter to summer over the subtropical East Asian sector occurs in late April. So defined, the mean onset date of EASSM is earlier than the mean onset of both the South China Sea summer monsoon (twenty-eighth pentad; Lau and Yang 1997; Wu and Zhang 1998) and the Indochinese Peninsula summer monsoon (9 May, or twenty-sixth pentad; Zhang et al. 2002).

As discussed in Zhao et al. (2007), seasonal transition over subtropical East Asia is likely a continuous process, which, if viewed in terms of surface wind reversal or local precipitation enhancement, may begin as early as the sixth pentad. We acknowledge the subjectivity of an EASSM onset index based primarily on the reversal of the meridional mean circulation over such a narrowly specified EASSM domain. Nevertheless, the evolution of the meridional wind circulation following a so-defined EASSM onset is generally consistent with that found in previous studies (Zhao et al. 2007; Zhu et al. 2012). In the meantime, the EASSM onset date so defined is also coincident with the mean reversal of the surface wind and zonal temperature deviation (gradient) averaged over this subtropical region, along with enhanced precipitation (Fig. 2).

Based on the above definition, the EASSM onset date (in pentads) for each year from 1979 to 2010 is determined (Table 1). The mean onset date is the twenty-third pentad,[2] with a standard deviation of 2.8 pentads. There are 14 and 13 years prior to and after this mean onset date, respectively. The year of earliest onset is 2008: transition begins on the fifteenth pentad (mid-March), though the domain-averaged precipitation is less than 5 mm day^{-1}at this time. The years of latest onset are 1981, 1983, 1989, and 2010, each with onset in the twenty-sixth pentad (early May). Onset is atypical for those years with an asterisk in Table 1, as the vertical meridional circulation is unsteady during the seasonal transition and may have, in fact, reversed directions multiple times. For example, in 1981, though the vertical meridional wind shear first reverses sign and the domain-averaged precipitation first exceeds 6 mm day^{-1} in the fifteenth pentad, the EASSM meridional cell is eventually established at the twenty-sixth pentad when the meridional shear reversal is accompanied in a reversal of the zonal temperature deviation (not shown).

Figures 5a–d show the composite mean of the meridional circulation at one pentad prior to, the pentad of,

[2] The number is one less than the climatological onset pentad, primarily because the mean onset date is an average of individual onset dates in the integer pentad, and the climatological onset date is the first integer pentad after the onset. Existence of the non-typical onset years, as well as the nonlinearity in the onset, may also contribute to this small difference.

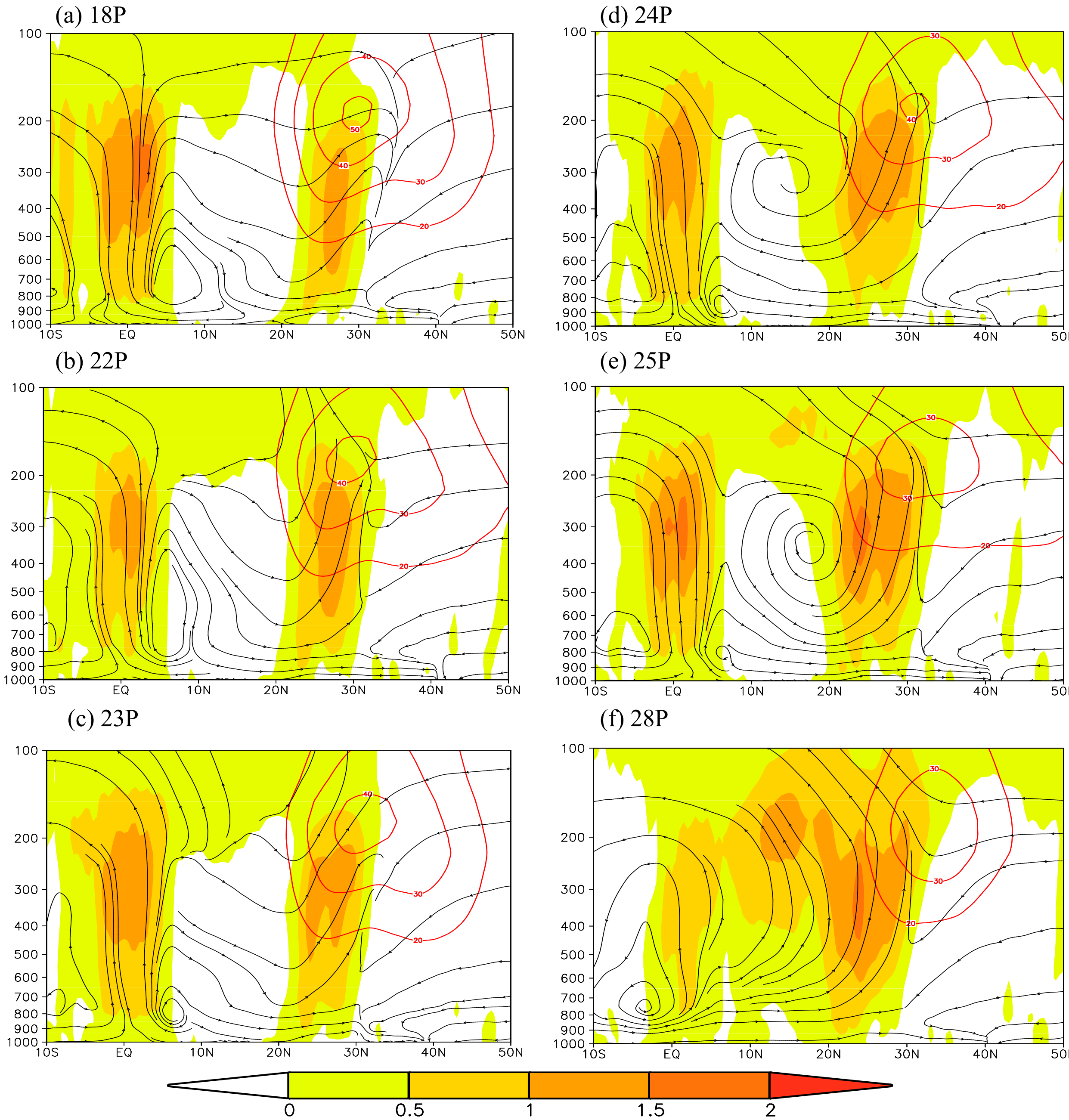

FIG. 3. Height–latitude cross section of the mean meridional circulation averaged over the East Asian sector (110°–120°E) at the (a) eighteenth, (b) twenty-second, (c) twenty-third, (d) twenty-fourth, (e) twenty-fifth, and (f) twenty-eighth pentads. Ascending vertical motion is shaded while zonal wind is contoured at 5 m s^{-1} intervals.

one pentad after, and two pentads after onset (expressed as pentads −1, 0, +1, and +2). These onset-relative composites illustrate a similar flow transition before and after EASSM onset seen in the climatological means in Figs. 3 and 4. The composite analysis shows a narrower and stronger Ferrel-like meridional cell centered at 300–400 hPa and 20°N. After onset (Figs. 5b–d), the meridional mean flow reverses direction more abruptly over the subtropical East Asian sector (20°–30°N). The abrupt flow transition during EASSM onset can also be clearly observed in the composite mean of the horizontal circulation at 200 hPa shown in Figs. 5e–h. Along with an eastward shift and weakening of the East Asian subtropical jet during EASSM onset, the SAH begins to reestablish itself from east of the Philippines (5°N, 160°E) to over the Indochinese Peninsula (10°N, 105°E)

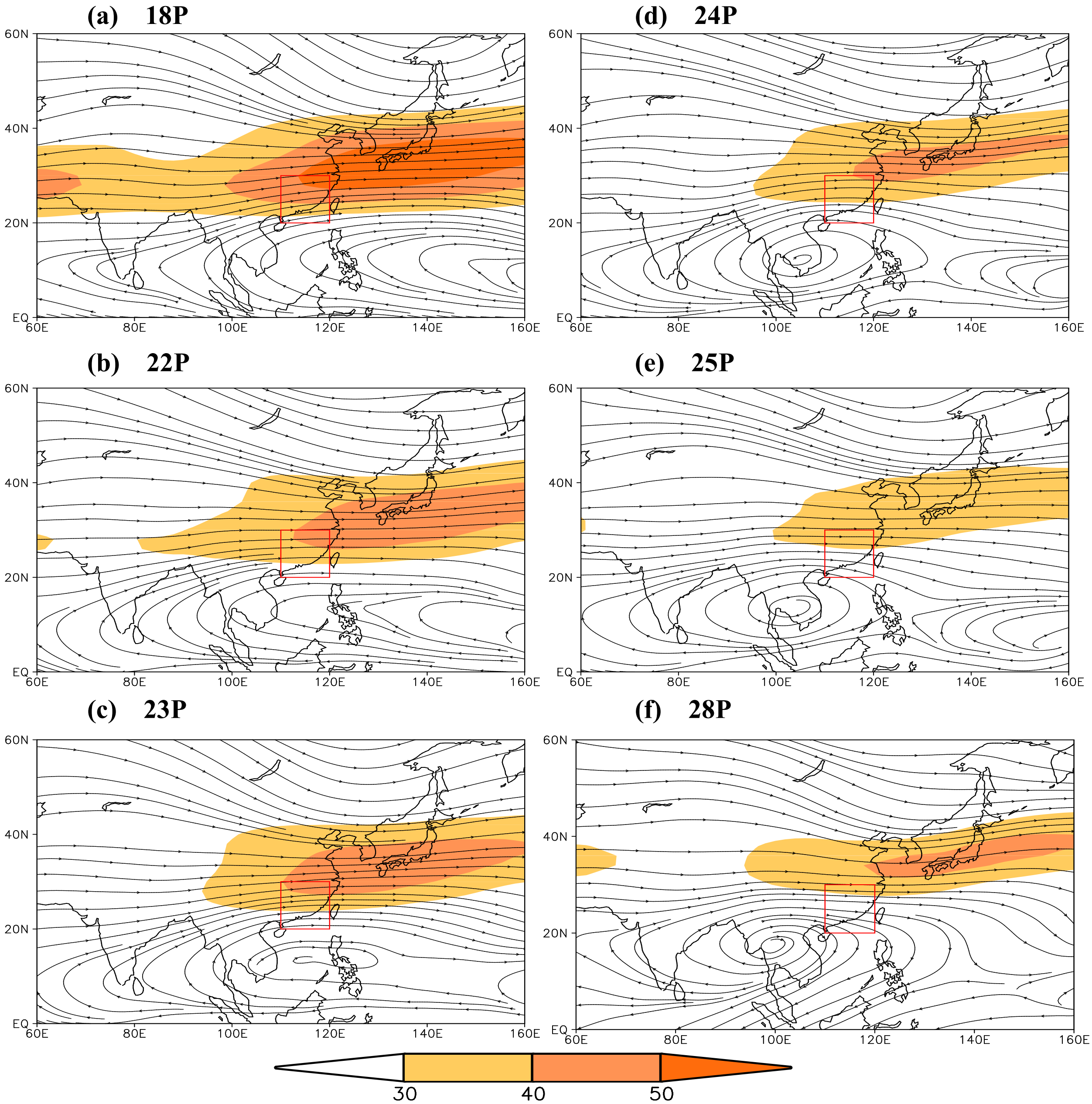

FIG. 4. As in Fig. 3, but for the 200-hPa wind field (streamlines, m s^{-1}). Zonal wind greater than 30 m s^{-1} is shaded.

(thereafter, the SAH continues a westward and northward propagation until it prevails over the Tibetan Plateau). This nearly 50° longitudinal shift of the SAH center changes the horizontal mean flow over the EASSM region from southwesterly (to the left of the SAH center) to northwesterly (to the right of the SAH), which is likely the primary reason for the vertical meridional mean-flow reversal during the EASSM onset.

The precise mechanisms that lead to the abrupt shift of SAH during the EASSM onset are beyond the scope of the current study. Previous studies of Li and Yanai (1996) and Minoura et al. (2003) showed that formation of the SAH is at least partly connected with intensified tropical convection in the vicinity of the Maritime Continent. Liu et al. (2009) also attributed the shift to the variation of the diabatic heating over the southern Asian subcontinent. The reversal of the zonal-mean temperature deviation during the climatological EASSM onset period is also evident in Fig. 2d. Since tropical convection and the associated low-frequency response have been identified to greatly influence the EASM (Zhou and Chan 2005, 2013; Straub et al. 2006; Tong et al. 2009;

TABLE 1. The EASSM onset date (Julian pentad) for each year from 1979 to 2010. The atypical onset years are denoted with an asterisk; these years are not used in the onset-relative composite analysis in Figs. 8–10.

Year	Onset date	Year	Onset date	Year	Onset date	Year	Onset date
1979*	23	1987	24	1995	24	2003	24
1980	19	1988	22	1996*	21	2004	23
1981*	26	1989	26	1997	25	2005	24
1982	23	1990	21	1998	23	2006	21
1983	26	1991	19	1999	20	2007*	25
1984	19	1992	18	2000*	23	2008*	15
1985*	19	1993	25	2001*	19	2009	20
1986	25	1994	20	2002	24	2010	26
Mean	23						

Li et al. 2013), the following section examines the likely linkage of the tropical MJO activities to the shift of SAH and the EASSM onset.

4. Potential linkage between MJO and EASSM onset

To examine the evolution of tropical convective activity on the intraseasonal time scale during the period of EASSM onset, Fig. 6 shows the onset-relative composite of the OLR pentad anomalies as a proxy of deep tropical convection. The pentad anomaly for each year is calculated by subtracting the corresponding 1981–2010 climatological mean without filtering. At pentad −3 (−3P), convective activity is suppressed over the entire tropical Indian Ocean (convection enhancement is observed over western Africa at −3P, not shown). Enhanced (suppressed) convective activity subsequently propagates eastward, reaching eastern Africa (eastern Indian Ocean and Maritime Continent) at −2P (Fig. 6b). The deep convection further propagates eastward to the western and central Indian Ocean by −1P, accompanied by positive MJO anomalies (indicating suppressed convection) over the Maritime Continent and western Pacific (Fig. 6c). The EASSM is established (0P, Fig. 6d) during the arrival of the enhanced convective activity over the central and eastern Indian Ocean (statistically significant at the 95% confidence level) and while the suppressed convection phase prevails over the western Pacific sector. Subsequently, the enhanced convective activity propagates eastward to the eastern Indian Ocean and the Maritime Continent by +1P, arriving at the western Pacific at +2P. In essence, Fig. 6 shows that the onset of EASSM is intimately associated with the evolution of deep tropical convection.

To further explore the linkage between the EASSM onset and MJO, the real-time multivariate MJO (RMM) index developed by Wheeler and Hendon (2004) (available online at http://www.cawcr.gov.au/staff/mwheeler/maproom/RMM/) is used here to identify different phases of MJOs during the EASSM onset for each of the 32 years. As shown in Fig. 7, the EASSM onset is strongly favored when the wet phases of the tropical MJO propagate from the western Indian Ocean to the central and eastern Indian Ocean. Nearly 70% of EASSM onset events (22 of 32 years) occur when MJO is active during phases 1–3; in particular, wet phases 2 and 3 are occurring for half of the onset events.

The potential influence of the MJO on the timing of the EASSM onset is further illustrated through the time–longitude Hovmöller diagrams of the composite[3] OLR anomalies along with the corresponding MJO-filtered signals from −6P to +6P averaged over the latitude bands of 15°S–15°N (Fig. 8a) and 20°–30°N (Fig. 8b), respectively. Consistent with what is shown in Figs. 6 and 7, the onset of EASSM (0P) starts when deep moist convection (reflected by the minimum OLR anomaly) in the tropics is propagating eastward from 40°E to 80°–100°E (Figs. 8a,c–h, with statistical significance exceeding the 95% confidence level). There are also eastward-propagating convective activities associated with the tropical MJO in the subtropical regions of the Northern Hemisphere. However, the eastward propagation of such intraseasonal convective activities in the subtropics is mostly stalled before reaching the Indochina region (90°–120°E) prior to EASSM onset (Figs. 8b,d–f).

It is beyond the scope of the current study to also fully explain the complex spatial patterns of the MJO-filtered signals and the interactions between the tropical and subtropical intraseasonal convective activities (Figs. 8c–h). Nevertheless, we further apply the same spatial–temporal MJO-filtering to the anomalies of other atmospheric variables that include horizontal wind, geopotential height, and air temperature represented by the corresponding CFS Reanalysis (only the 24 years of typical EASSM onset are used for the composite). The time–height Hovmöller diagrams composited relative to the EASSM onset pentad (Figs. 9a,c,e) show that both of the original and the MJO-filtered anomalies of these three variables averaged over the EASSM domain are maximized in the upper troposphere (around 200 hPa for meridional winds and geopotential heights and around 300 hPa for temperature). Most notably, the MJO-filtered upper-tropospheric meridional wind anomalies shift from being distinctly positive (southerly) to negative (northerly) just before the EASSM onset (Figs. 9e,f), suggesting

[3] Only the 24 typical onset events (denoted in Table 1) were included in the composite analysis of Figs. 8–10, though the results would be qualitatively similar if all 32 years were used (not shown).

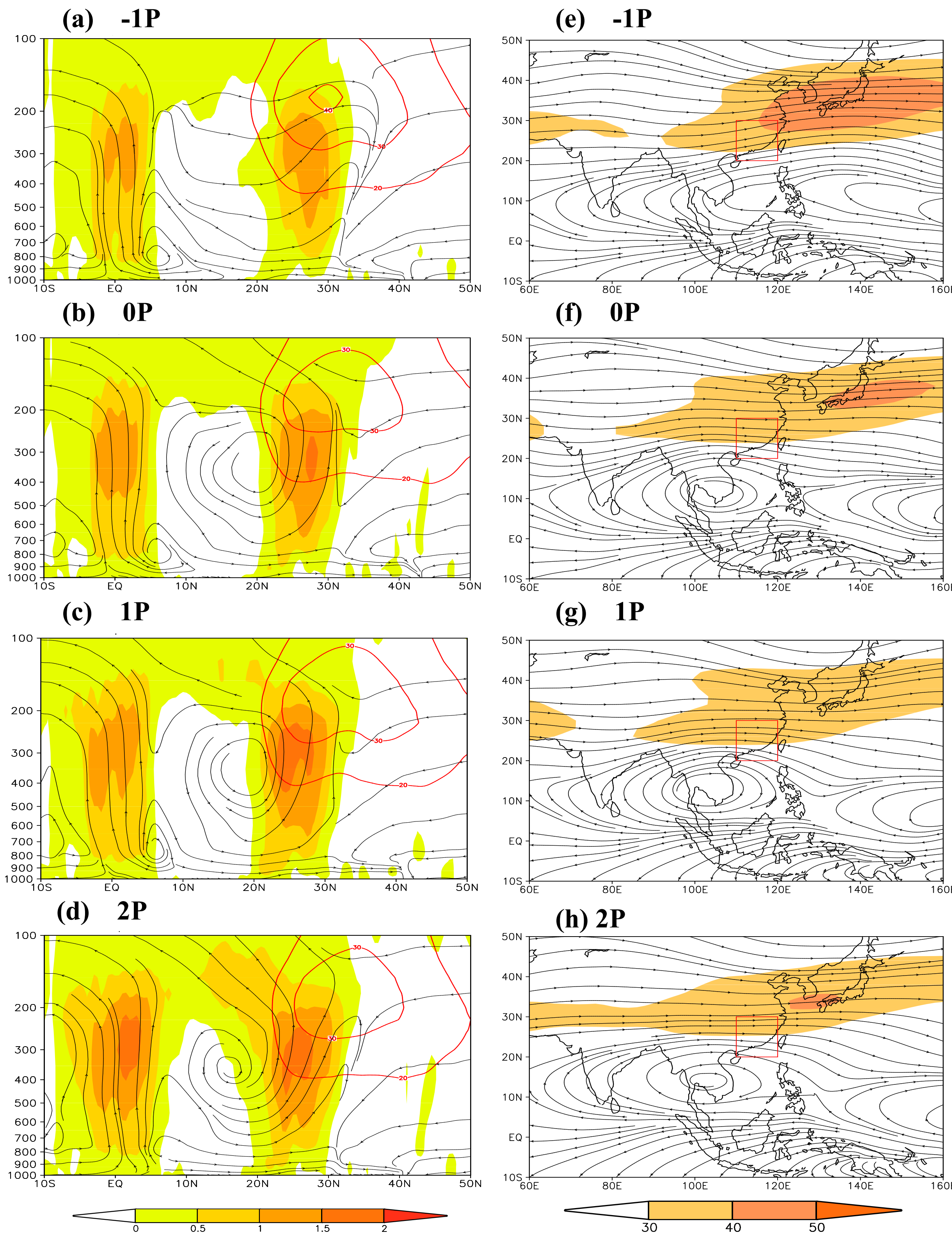

FIG. 5. (a)–(d) As in Fig. 3, but for the onset-relative composites from −1P to +2P. (e)–(h) As in Fig. 4, but for the onset-relative composites from −1P to +2P.

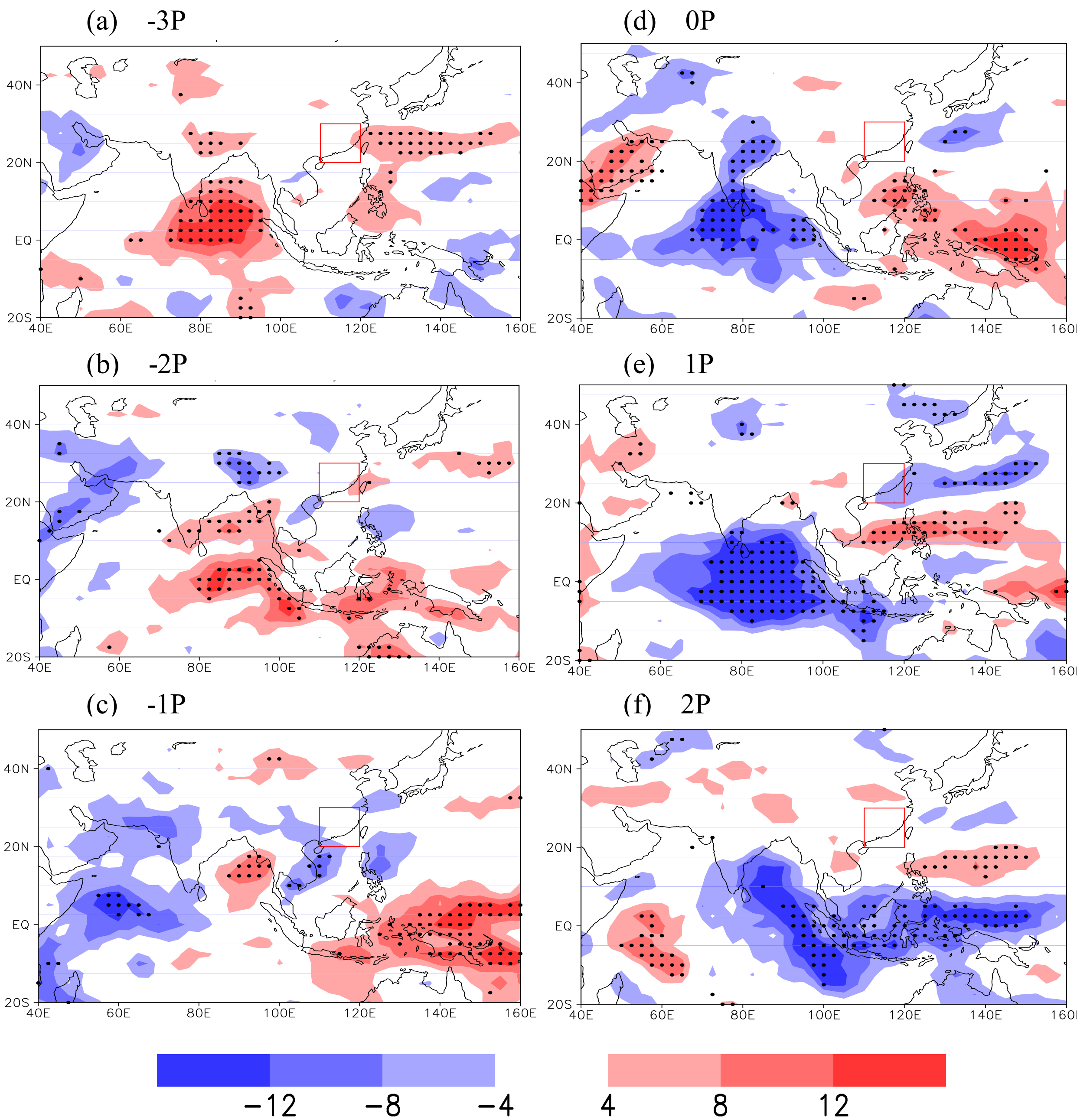

FIG. 6. The onset-relative composite OLR (W m^{-2}) anomalies from −3P to +2P. Negative values indicate deep convection. The red rectangle denotes the EASSM domain. Stippling indicates statistical significance at the 95% level.

a strong connection between the tropical MJO and the upper-tropospheric meridional wind reversal (a key factor in defining the EASSM onset). The MJO-filtered height and temperature anomalies over the subtropics are predominantly negative prior to the EASSM onset, then change to positive soon after the onset (Figs. 9a,c). Again, while it is beyond the scope of the current study to examine how precisely the tropical MJO may be responsible for these negative height and temperature anomalies in the subtropics, changes in these height and temperature anomalies will impact the meridional wind reversal as evidenced from Figs. 9f and 10k–o. Note, as expected, the MJO-filtered height, temperature, and wind anomalies in the upper troposphere are much stronger in the subtropics than in the tropics (Figs. 9 and 10). The MJO-filtered convective activities represented by OLR, on the other hand, are maximized in the tropics (Fig. 8).

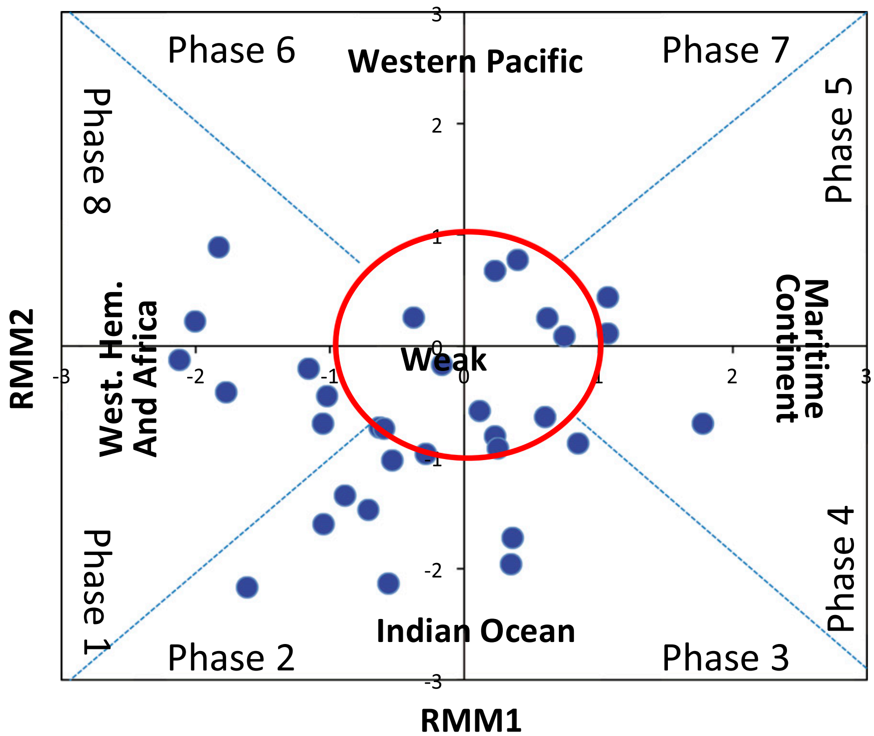

FIG. 7. Phase-space diagram of MJO according to the RMM index of Wheeler and Hendon (2004) for each year from 1979 to 2010.

Given the composite analysis in Fig. 5 showing that the onset of the EASSM (and the meridional wind reversal over subtropical East Asia) is directly linked to an abrupt longitudinal shift of the SAH (from being centered at 160° to around 105°E for −1P and 0P, respectively, though varying slightly between different levels), it is natural to ask how the tropical MJO may potentially impact this westward shift of SAH. Indeed, these MJO-filtered negative height anomalies are at least consistent with (if not directly responsible for) the westward shift of the SAH center. For example, at −2P, there are strong negative (moderate positive) MJO-filtered height anomalies to the west (east) of the East Asia subtropical sector (red box, Fig. 10a). The strong negative MJO-filtered height anomalies shift to being maximized just to the east of the subtropical domain after the EASSM onset, while moderate positive anomalies developed to the west (Fig. 10c), which is consistent with the shifting of the SAH from being centered to the east to being centered to the west of the focus subtropical domain before and after the onset of EASSM (Figs. 5e–g and 10b–d).

The positive anomalous pairs prevailing over the subtropics around 40°–50°E move eastward during EASSM onset, accompanying the eastward propagation of strong negative height anomalies (0P, Fig. 10c). This pattern is consistent with the Rossby wave response to the MJO heating (Rui and Wang 1990; Hendon and Salby 1994; Kiladis et al. 2005; Wu et al. 2006; Barlow 2011). In the upper troposphere, these anomalous cyclone–anticyclone pairs extend to the subtropics and interact with the climatological jet (Barlow et al. 2005; Barlow 2011; Hoell et al. 2012; Adames and Wallace 2014). The propagating Rossby "gyres" exhibit larger amplitudes in the geopotential height and temperature fields than the equatorial Kelvin waves, as found in the current study (Figs. 9 and 10).

Moreover, Figs. 10a–j also shows that the MJO-filtered height anomalies are highly correlated with the MJO-filtered temperature anomalies. This correlation is generally consistent with Hoell et al. (2012), who proposed that the temperature advection contributes to the anomalous ascent over South Asia at both the intraseasonal and interannual time scales. Yang et al. (2007) also showed that warming over the Indian Ocean basin may lead to strengthening of the SAH through the Matsuno–Gill-like response (Matsuno 1966; Gill 1980). Since the EASSM onset can be identified by the reversal of the meridional mean circulation (particularly due to wind direction changes in the upper troposphere) over the East Asian subtropical sector, the above analysis shows that it is strongly associated with MJO-related height and temperature anomalies. Although it is beyond the scope of the current study to pinpoint the exact dynamics, our analysis suggests that the tropical MJO activity may potentially be

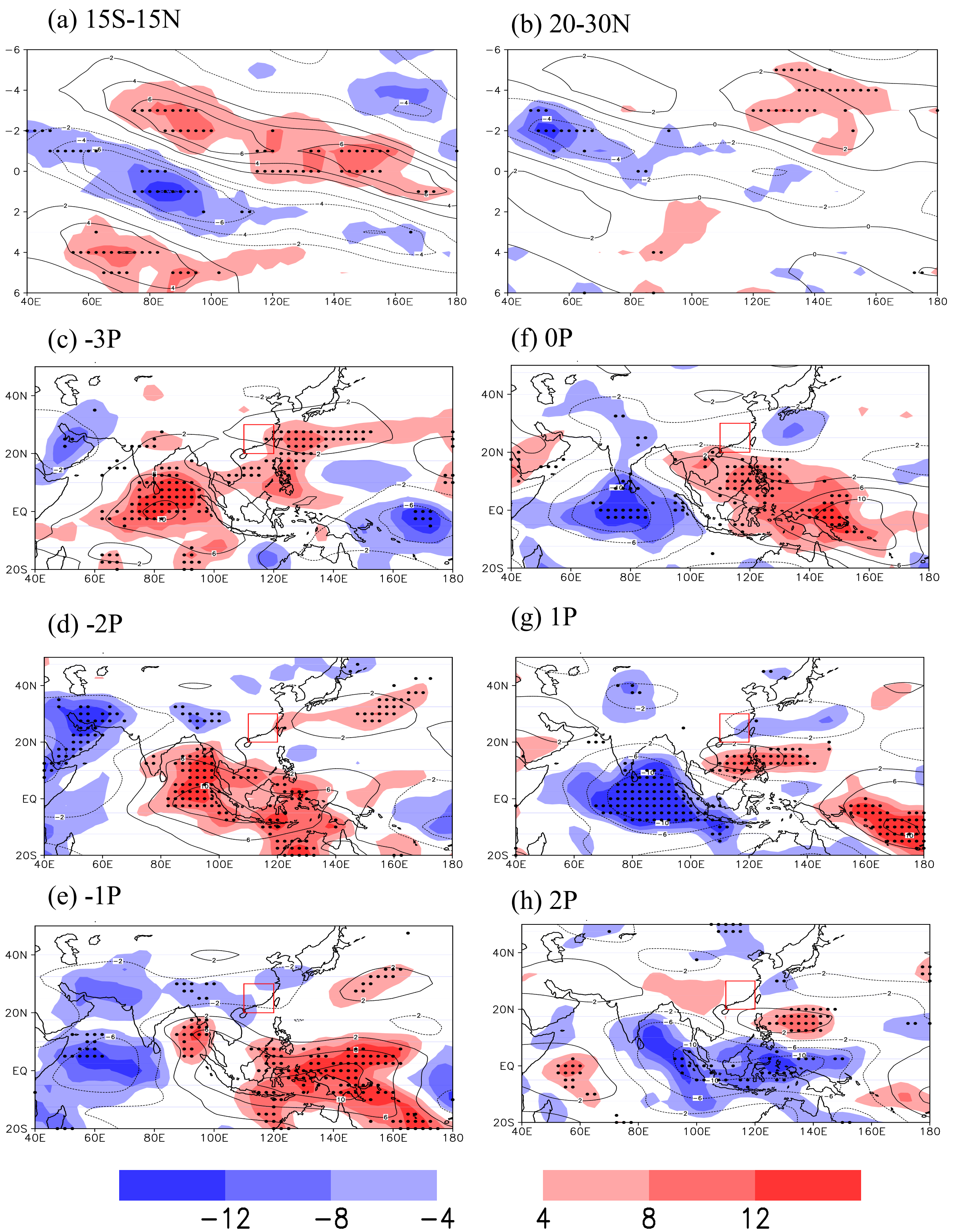

FIG. 8. (a),(b) Longitude–time Hovmöller diagram of the composite OLR anomalies (shaded, W m^{-2}) and the MJO-filtered band (contoured, W m^{-2}) from −6P to +6P averaged over 15°S–15°N and 20°–30°N, respectively. (c)–(h) Composite OLR anomalies (shaded, W m^{-2}) and the MJO-filtered anomalies (contoured, W m^{-2}) from −3P to +2P, respectively. Areas with statistical significance over the 95% confidence level are stippled.

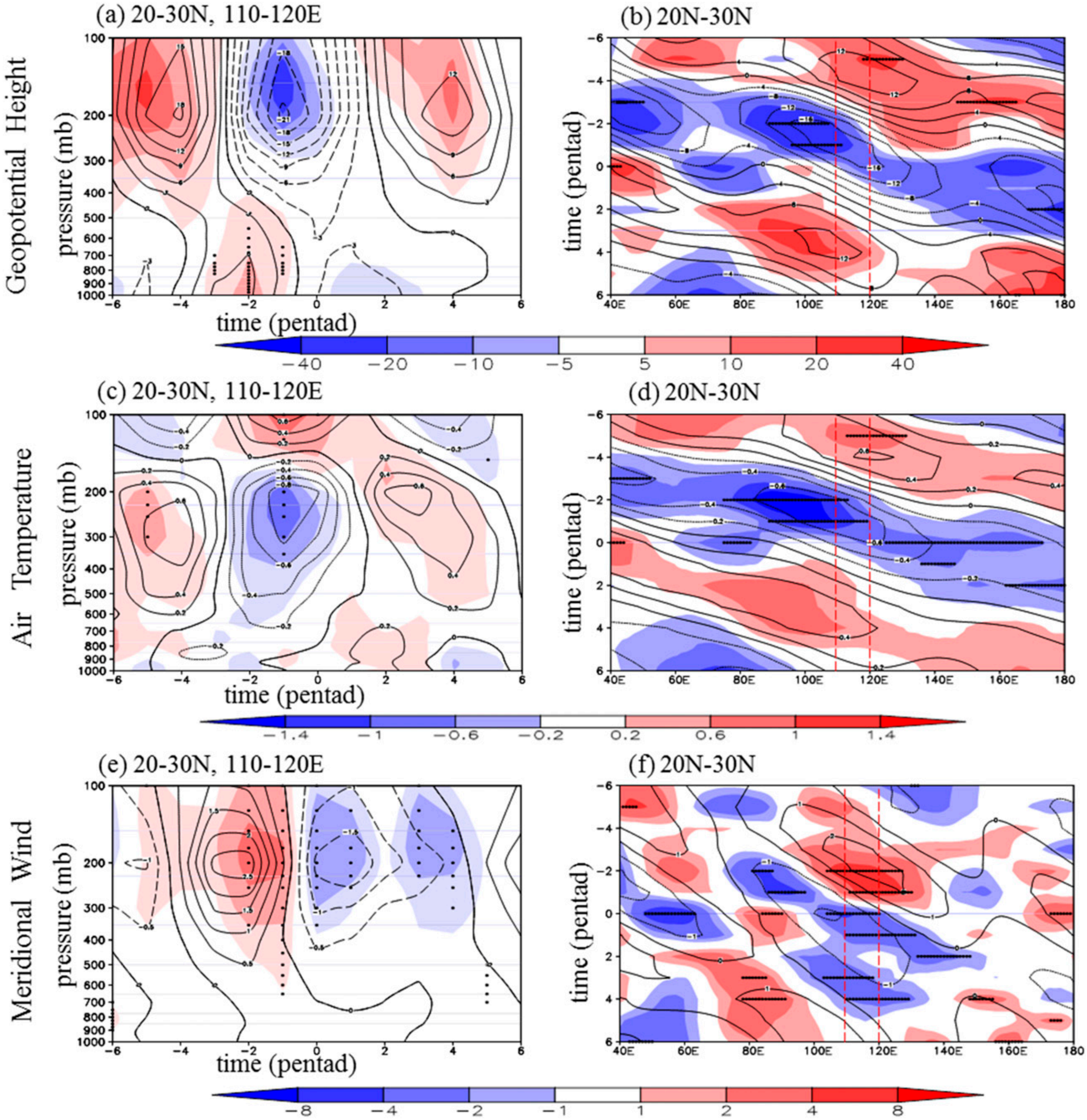

FIG. 9. (a),(c),(e) Height–time Hovmöller diagrams of anomalies of geopotential height (gpm), temperature (K), and meridional wind ($m\,s^{-1}$) (shaded), respectively, and the MJO-filtered anomalies (contours) averaged over the EASSM region. (b),(d),(f) Longitude–time Hovmöller diagrams of anomalies of composite 200-hPa height, 300-hPa temperature, and 200-hPa meridional wind (shaded, averaged over 20°–30°N), respectively, and the MJO-filtered band (contours). Areas with statistical significance over the 95% confidence level are stippled.

one of the important factors that contribute to the EASSM onset.

5. Concluding remarks

The current study examines the characteristics of changes in the atmospheric circulation associated with the onset of EASSM and the correlation between the tropical MJO activities and the EASSM onset. The climatological onset of EASSM, signaling the seasonal transition from winter to summer over East Asia, occurs on the twenty-fourth pentad, when there is a reversal of meridional wind in the upper troposphere. The reversal of the focus-domain-averaged vertical meridional wind

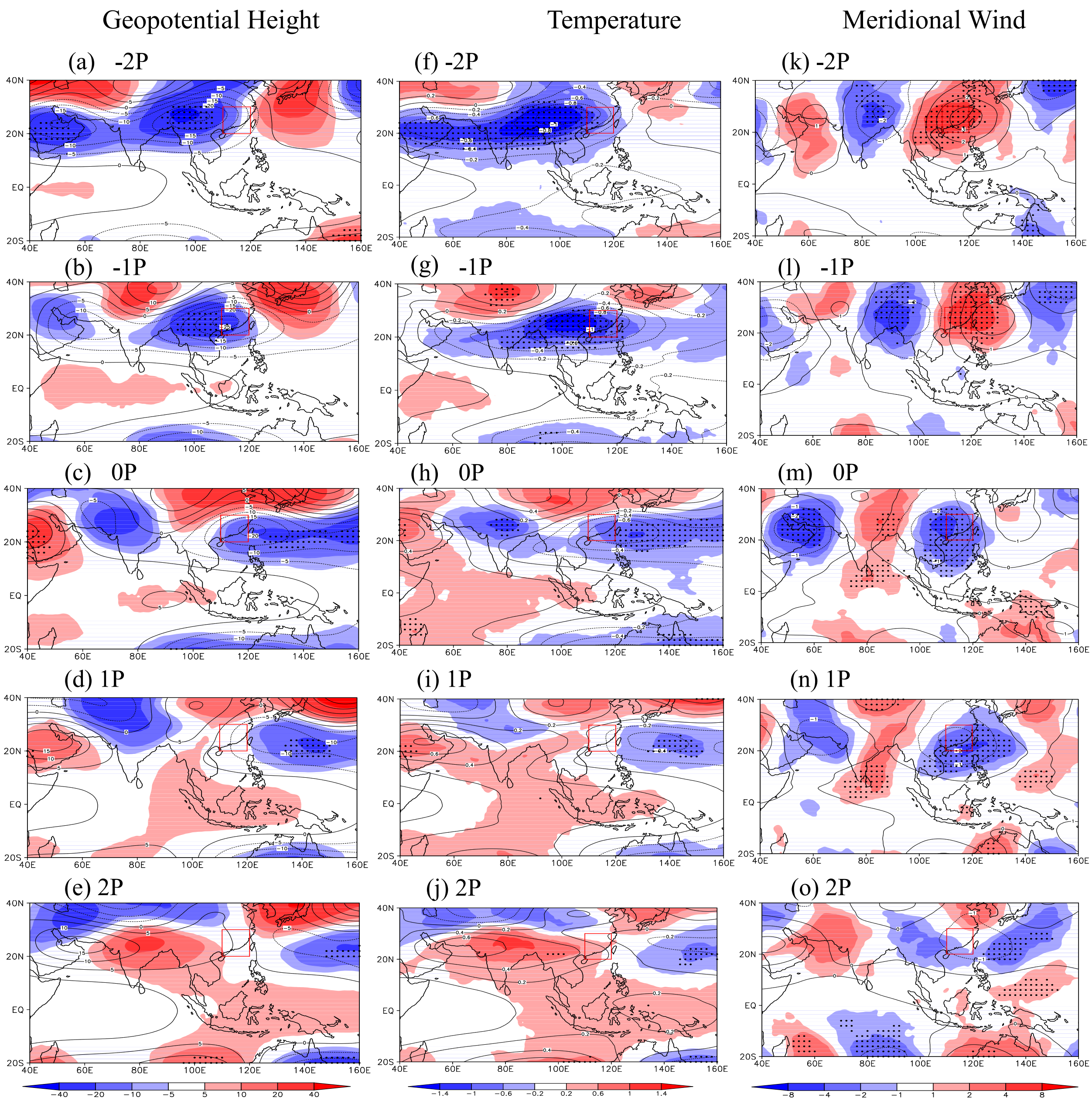

FIG. 10. Composite (shaded) and MJO-filtered anomalies (contoured) from −2P to +2P for (a)–(e) 200-hPa geopotential height (gpm), (f)–(j) 300-hPa air temperature (K), and (k)–(o) 200-hPa meridional wind ($m\,s^{-1}$). Areas with statistical significance over the 95% confidence level are stippled.

shear is thus used as a key index to define the EASSM onset date for each year based on the CFS Reanalysis. The mean onset date of the EASSM occurs during the twenty-third pentad with a standard deviation of 2.8 pentads. The onset-relative composite analysis indicates that the vertical meridional flow reversal is most likely attributable to the reestablishment of SAH over the southern Indochinese Peninsula after an abrupt westward shift in the upper troposphere.

Further analysis reveals that the onset of the EASSM and the reestablishment of SAH are associated with the eastward propagation of the wet phase of the tropical MJO from the western Indian Ocean to the eastern Indian Ocean. It is suggested that the tropical MJO may be strongly linked to the westward shift of SAH, which causes the reversal of MJO-filtered meridional wind anomalies associated with the EASSM onset.

However, the tropical MJO activities may not be the only factor to the EASSM onset. It remains unclear what causes the convection's eastward movement that affects the convective development in the East Asian subtropical region. Previous works also showed the potential impact of midlatitude systems on the EASM onset (e.g., Chang and Chen 1995; Ding and Liu 2001), as well as the initiation of tropical MJOs (e.g., Zhang 2013). Meanwhile, the heating impact of the Tibetan Plateau and the midlatitude baroclinic systems may have also contributed to EASSM onset, which is beyond the scope of the current research.

Moreover, the current results are obtained primarily through composite observational analysis of historical atmospheric records. Future research is also needed to further establish the potential causation and the likely underlying mechanisms, possibly with the aid of numerical sensitivity experiments.

Acknowledgments. The authors are grateful for the editor, three anonymous reviewers, and Scott Sieron for their constructive comments and suggestions. This research is supported by the National Basic Research Program of China (973 Program, Grant 2013CB430202), National Department Public Benefit Research Foundation of China (Grant GYHY201306032), and the U.S. National Science Foundation (Grant 1305798).

REFERENCES

Adames, A. F., and J. M. Wallace, 2014: Three-dimensional structure and evolution of the MJO and its relation to the mean flow. *J. Atmos. Sci.,* **71,** 2007–2026, doi:10.1175/JAS-D-13-0254.1.

Barlow, M., 2011: The Madden–Julian Oscillation influence on Africa and West Asia. *Intraseasonal Variability of the Atmosphere–Ocean–Climate System,* 2nd ed. W. K. M. Lau and D. E. Waliser, Eds., Springer Praxis, 477–493.

——, M. Wheeler, B. Lyon, and H. Cullen, 2005: Modulation of daily precipitation over Southwest Asia by the Madden–Julian oscillation. *Mon. Wea. Rev.,* **133,** 3579–3594, doi:10.1175/MWR3026.1.

Chan, J. C.-L., Y.-G. Wang, and J.-J. Xu, 2000: Dynamic and thermodynamic characteristics associated with the onset of the 1998 South China Sea summer monsoon. *J. Meteor. Soc. Japan,* **78,** 367–380.

Chang, C.-P., and G. T.-J. Chen, 1995: Tropical circulations associated with southwest monsoon onset and westerly surges over the South China Sea. *Mon. Wea. Rev.,* **123,** 3254–3267, doi:10.1175/1520-0493(1995)123<3254:TCAWSM>2.0.CO;2.

——, Z. Wang, J.-H. Ju, and T. Li, 2004: On the relationship between western Maritime Continent monsoon rainfall and ENSO during northern winter. *J. Climate,* **17,** 665–672, doi:10.1175/1520-0442(2004)017<0665:OTRBWM>2.0.CO;2.

Chen, L.-X., W. Li, P. Zhao, and S.-Y. Tao, 2000: Process of summer monsoon onset in eastern Asia (in Chinese). *Res. Climate Environ.,* **5,** 345–355.

Ding, Y.-H., 1994: *Monsoons over China.* Kluwer Academic Publishers, 420 pp.

——, and Y.-J. Liu, 2001: Onset and the evolution of the Summer Monsoon over the South China Sea during SCSMEX field experiment in 1998. *J. Meteor. Soc. Japan,* **79,** 255–276, doi:10.2151/jmsj.79.255.

——, and J. C.-L. Chan, 2005: The East Asian summer monsoon: An overview. *Meteor. Atmos. Phys.,* **89,** 117–142, doi:10.1007/s00703-005-0125-z.

Gill, A. E., 1980: Some simple solutions for heat-induced tropical circulation. *Quart. J. Roy. Meteor. Soc.,* **106,** 447–462, doi:10.1002/qj.49710644905.

He, J.-H., L. Qi, J. Wei, and Y.-Z. Chi, 2007: Reinvestigations on the East Asian subtropical monsoon and tropical monsoon (in Chinese). *Chin. J. Atmos. Sci.,* **31,** 1257–1265.

——, P. Zhao, C. Zhu, R. Zhang, X. Tang, L. Chen, and X. Zhou, 2008: Discussion of some problems as to the East Asian Subtropical monsoon (in Chinese). *Acta Meteor. Sin.,* **66,** 419–434.

Hendon, H. H., and M. L. Salby, 1994: The life cycle of the Madden–Julian Oscillation. *J. Atmos. Sci.,* **51,** 2225–2237, doi:10.1175/1520-0469(1994)051<2225:TLCOTM>2.0.CO;2.

Hoell, A., M. Barlow, and R. Saini, 2012: The leading pattern of intraseasonal and interannual Indian Ocean precipitation variability and its relationship with Asian circulation during the boreal cold season. *J. Climate,* **25,** 7509–7526, doi:10.1175/JCLI-D-11-00572.1.

Kiladis, G. N., K. H. Straub, and P. T. Haertel, 2005: Zonal and vertical structure of the Madden–Julian Oscillation. *J. Atmos. Sci.,* **62,** 2790–2809, doi:10.1175/JAS3520.1.

Lau, W. K.-M., and S. Yang, 1997: Climatology and interannual variability of the Southeast Asian summer monsoon. *Adv. Atmos. Sci.,* **14,** 141–162, doi:10.1007/s00376-997-0016-y.

——, and D. E. Waliser, 2012: *Intraseasonal Variability in the Atmosphere–Ocean Climate System*. 2nd ed. Springer, 613 pp.

Li, C., and M. Yanai, 1996: The onset and interannual variability of the Asian summer monsoon in relation to land–sea thermal contrast. *J. Climate,* **9,** 358–375, doi:10.1175/1520-0442(1996)009<0358:TOAIVO>2.0.CO;2.

Li, T., X.-Q. Yang, and J.-H. Ju, 2013: Intraseasonal oscillation features of the South China Sea summer monsoon and its response to abnormal Madden and Julian Oscillation in the tropical Indian Ocean. *Sci. China Earth Sci.,* **56,** 866–877, doi:10.1007/s11430-012-4521-1.

Liebmann, B., and C. A. Smith, 1996: Description of a complete (interpolated) outgoing longwave radiation dataset. *Bull. Amer. Meteor. Soc.,* **77,** 1275–1277.

Liu, B.-Q., J.-H. He, and L.-J. Wang, 2009: Characteristics of the South Asia high establishment processes above the Indo-China Peninsula from April to May and their possible mechanism (in Chinese). *Chin. J. Atmos. Sci.,* **33,** 1319–1332, doi:10.3878/j.issn.1006-9895.2009.06.17.

Madden, R. A., and P. R. Julian, 1971: Detection of a 40–50 day oscillation in the zonal wind in the tropical Pacific. *J. Atmos. Sci.,* **28,** 702–708, doi:10.1175/1520-0469(1971)028<0702:DOADOI>2.0.CO;2.

Matsuno, T., 1966: Quasi-geostrophic motions in the equatorial area. *J. Meteor. Soc. Japan,* **44,** 25–43.

Minoura, D., R. Kawamura, and T. Matsuura, 2003: A mechanism of the onset of the South Asian summer monsoon. *J. Meteor. Soc. Japan,* **81,** 563–580, doi:10.2151/jmsj.81.563.

Qi, L., J.-H. He, Z.-Q. Zhang, and J.-N. Song, 2008: Seasonal cycle of the zonal land–sea thermal contrast and East Asian subtropical monsoon circulation (in Chinese). *Chin. Sci. Bull.,* **53,** 131–136, doi:10.1007/s11434-007-0518-0.

Qian, W.-H., and D.-K. Lee, 2000: Seasonal march of Asian summer monsoon. *Int. J. Climatol.,* **20,** 1371–1386, doi:10.1002/1097-0088(200009)20:11<1371::AID-JOC538>3.0.CO;2-V.

Qian, Y.-F., Y. Zhang, J. Jiang, Y. Yao, and Z. Xu, 2005: The earliest onset areas and mechanism of the tropical Asian summer monsoon. *Acta Meteor. Sin.,* **19,** 129–142.

Ren, K., J.-H. He, and L. Qi, 2010: The establishment characteristics of the East Asian subtropical monsoon rain belt and an analysis of its nature of precipitation (in Chinese). *Acta Meteor. Sin.,* **68,** 550–558.

Rui, H., and B. Wang, 1990: Development characteristics and dynamic structure of tropical intraseasonal convection anomalies. *J. Atmos. Sci.,* **47,** 357–379, doi:10.1175/1520-0469(1990)047<0357:DCADSO>2.0.CO;2.

Saha, S., and Coauthors, 2010: The NCEP Climate Forecast System Reanalysis. *Bull. Amer. Meteor. Soc.,* **91,** 1015–1057, doi:10.1175/2010BAMS3001.1.

Straub, K. H., G. N. Kiladis, and P. E. Ciesielski, 2006: The role of equatorial waves in the onset of the South China Sea summer monsoon and the demise of El Niño during 1998. *Dyn. Atmos. Oceans,* **42,** 216–238, doi:10.1016/j.dynatmoce.2006.02.005.

Tao, S.-Y., and L.-X. Chen, 1987: A review of recent research on the East Asian summer monsoon in China. *Monsoon Meteorology,* C. P. Chang and T. N. Krishnamurti, Eds., Oxford University Press, 60–92.

Tian, S.-F., and T. Yasunari, 1998: Climatological aspects and mechanism of spring persistent rains over central China. *J. Meteor. Soc. Japan,* **76,** 57–71.

Tong, H.-W., J. C. L. Chan, and W. Zhou, 2009: The role of MJO and mid-latitude fronts in the South China Sea summer monsoon onset. *Climate Dyn.,* **33,** 827–841, doi:10.1007/s00382-008-0490-7.

Wan, R.-J., and G.-X. Wu, 2007: Mechanism of the spring persistent rains over southeastern China. *Sci. China,* **50D,** 130–144, doi:10.1007/s11430-007-2069-2.

Wang, B., and LinHo, 2002: Rainy season of the Asian–Pacific summer monsoon. *J. Climate,* **15,** 386–398, doi:10.1175/1520-0442(2002)015<0386:RSOTAP>2.0.CO;2.

——, R.-G. Wu, and X.-H. Fu, 2000: Pacific–East Asian teleconnection: How does ENSO affect East Asian climate? *J. Climate,* **13,** 1517–1536, doi:10.1175/1520-0442(2000)013<1517:PEATHD>2.0.CO;2.

——, LinHo, Y.-S. Zhang, and M.-M. Lu, 2004: Definition of South China Sea monsoon onset and commencement of the East Asia summer monsoon. *J. Climate,* **17,** 699–710, doi:10.1175/2932.1.

Wen, Z.-P., H.-Y. He, and R.-H. Huang, 2004: The influence of 30∼60 d oscillation on the development of the South China Sea summer monsoon. *Acta Oceanol. Sin.,* **23,** 569–579.

Wheeler, M. C., and G. N. Kiladis, 1999: Convectively coupled equatorial waves: Analysis of clouds in the wavenumber–frequency domain. *J. Atmos. Sci.,* **56,** 374–399, doi:10.1175/1520-0469(1999)056<0374:CCEWAO>2.0.CO;2.

——, and H. H. Hendon, 2004: An all-season real-time multivariate MJO index: Development of an index for monitoring and prediction. *Mon. Wea. Rev.,* **132,** 1917–1932, doi:10.1175/1520-0493(2004)132<1917:AARMMI>2.0.CO;2.

Wu, G.-X., and Y.-S. Zhang, 1998: Tibetan Plateau forcing and the timing of the monsoon onset over South Asia and the South China Sea. *Mon. Wea. Rev.,* **126,** 913–927, doi:10.1175/1520-0493(1998)126<0913:TPFATT>2.0.CO;2.

——, Y. Liu, B. Dong, X. Liang, A. Duan, Q. Bao, and J. Yu, 2012: Revisiting Asian monsoon formation and change associated with Tibetan Plateau forcing: I. Formation. *Climate Dyn.,* **39,** 1169–1181, doi:10.1007/s00382-012-1334-z.

Wu, M. L. C., S. D. Schubert, M. J. Suarez, P. J. Pegion, and D. E. Waliser, 2006: Seasonality and meridional propagation of the MJO. *J. Climate,* **19,** 1901–1921, doi:10.1175/JCLI3680.1.

Xie, P.-P., and P. A. Arkin, 1997: Global precipitation: A 17-year monthly analysis based on gauge observations, satellite estimates, and numerical model outputs. *Bull. Amer. Meteor. Soc.,* **78,** 2539–2558, doi:10.1175/1520-0477(1997)078<2539:GPAYMA>2.0.CO;2.

Xu, G.-Q., and Q.-G. Zhu, 2002: Feature analysis of summer monsoon LFO over SCS in 1998 (in Chinese). *J. Trop. Meteor.,* **18,** 309–316.

Yang, J.-L., Q. Liu, S.-P. Xie, Z. Liu, and L. Wu, 2007: Impact of the Indian Ocean SST basin mode on the Asian summer monsoon. *Geophys. Res. Lett.,* **34,** L02708, doi:10.1029/2006GL028571.

Zhang, C.-D., 2013: Madden–Julian Oscillation: Bridging weather and climate. *Bull. Amer. Meteor. Soc.,* **94,** 1849–1870, doi:10.1175/BAMS-D-12-00026.1.

Zhang, Y.-S., T. L. B. Wang, and G. Wu, 2002: Onset of the summer monsoon over the Indochina Peninsula: Climatology and interannual variations. *J. Climate,* **15,** 3206–3221, doi:10.1175/1520-0442(2002)015<3206:OOTSMO>2.0.CO;2.

Zhang, Z.-Q., J. C.-L. Chan, and Y.-H. Ding, 2004: Characteristics, evolution and mechanisms of the summer monsoon onset over Southeast Asia. *Int. J. Climatol.,* **24,** 1461–1482, doi:10.1002/joc.1082.

Zhao, P., R. Zhang, J. Liu, X. Zhou, and J. He, 2007: Onset of southwesterly wind over eastern China and associated atmospheric circulation and rainfall. *Climate Dyn.,* **28,** 797–811, doi:10.1007/s00382-006-0212-y.

Zhou, W., and J. C.-L. Chan, 2005: Intraseasonal oscillations and the South China Sea summer monsoon onset. *Int. J. Climatol.,* **25,** 1585–1609, doi:10.1002/joc.1209.

——, and ——, 2013: Intraseasonal to interdecadal variations of South China Sea Summer Monsoon. *Geophysical Research Abstracts,* Vol. **15,** EGU13579. [Available online at http://meetingorganizer.copernicus.org/EGU2013/EGU2013-13579.pdf.]

Zhu, C.-W., X.-J. Zhou, P. Zhao, L.-X. Chen, and J.-H. He, 2011: Onset of East Asian subtropical summer monsoon and rainy season in China. *Sci. China Earth Sci.,* **54,** 1845–1853, doi:10.1007/s11430-011-4284-0.

Zhu, Q.-G., J.-H. He, and P.-X. Wang, 1986: A study of circulation differences between East-Asian and Indian summer monsoons with their interaction. *Adv. Atmos. Sci.,* **3,** 466–477, doi:10.1007/BF02657936.

——, J.-R. Lin, S.-W. Shou, and D.-S. Tang, 2000: *The Principle and Method of Weather* (in Chinese). China Meteorological Press, 914 pp.

Zhu, Z.-W., J.-H. He, and L. Qi, 2012: Seasonal transition of East Asian subtropical monsoon and its possible mechanism. *J Trop. Meteor.,* **18,** 305–313.